Electronic and vibronic structure of the $(GaAs)_1(AlAs)_1$ superlattice

M. Cardona, T. Suemoto,* N. E. Christensen, T. Isu,† and K. Ploog
Max-Planck-Institut für Festkörperforschung, Heisenbergstrasse 1, D-7000 Stuttgart 80, Federal Republic of Germany
(Received 16 December 1986; revised manuscript received 9 June 1987)

Resonant Raman scattering has been observed in $(GaAs)_1(AlAs)_1$ superlattices (one layer of GaAs alternating with one layer of AlAs) for the excitations in the region of the optical phonons of AlAs and GaAs with use of laser photon energies around 1.9 and 2.1 eV. With the help of linear muffin-tin-orbital (LMTO) band-structure calculations these resonances are attributed to transitions from the GaAs-like top of the valence band to the folded X_3 conduction band of AlAs and to the Γ_1 GaAs-like conduction band. The Raman spectra reveal longitudinal phonons propagating perpendicular to the superlattice planes and also, around the 1.9-eV resonance, satellites of these phonons shifted slightly to higher frequencies. These satellites are tentatively attributed to random inversion of Al-Ga pairs, i.e., to imperfections of the superlattice.

I. INTRODUCTION

The electronic structure of GaAs-AlAs-based superlattices has received considerable attention.[1-8] In order to avoid the complications involved in the electronic structure of the alloys, most calculations consider superlattices composed of n layers of pure AlAs alternating with m layers of GaAs [denoted $(GaAs)_m(AlAs)_n$]. We discuss here the prototype of those superlattices, namely that for $m=n=1$ (1×1).

For superlattices with large values of m and n [$m,n>4$ (Ref. 1)] the electronic structure near the GaAs-like band edges can be simplified with the concept of confinement. The electrons are confined to the GaAs slabs and can be treated as two dimensional. The calculation of the two-dimensional electron bands can be easily performed once the band offset at the interface is known. One has, in this case, a system of multiple quantum wells. For $m,n\leq4$, the interaction between the electrons in the quantum wells is considerable and the two-dimensional character is lost. The calculations must then be performed by treating the crystal as a whole, with a large primitive cell consisting of the $(GaAs)_m(AlAs)_n$ building block. Two types of such calculations have been performed. In Refs. 1, 4, and 6 the calculations were based on the empirical pseudopotentials of the constituent atoms which, unfortunately, are only reliably known for wave vectors $|\mathbf{G}|\geq(2\pi/a_0)\sqrt{3}$ (a_0=lattice constant of GaAs).[4] The pseudopotentials for smaller values of $|\mathbf{G}|$ can be obtained by extrapolation, so as to yield the correct band offset for $m,n>4$. The accuracy of such procedure is difficult to evaluate. The calculations of Ref. 2 were based on empirical tight binding parameters. Other calculations are *ab initio*, based on a self-consistent potential in which, however, exchange and correlation are treated in the local-density approximation (LDA).[3,7] This approximation is known to lead to errors in the gaps for interband excitations.[9] Several *ad hoc* methods are used to correct such errors, at least partially, by adjusting some parameters like α in the so-called X_α method,[3] or introducing a "scissors operator."[10]

In this paper we have tried to overcome this "gap problem" which arises in LDA calculations of $(GaAs)_1(AlAs)_1$ superlattices by adding external potentials which are sharply peaked at the centers of the spheres used in the LMTO calculations of Ref. 5. The strengths of these potentials were determined so as to correct the "gap problem" in the bulk constituents.[11] Although the accuracy of the procedure is also difficult to ascertain from the fact that it works on GaAs and AlAs, it is easy to conjecture that it should also work for $(GaAs)_1(AlAs)_1$. An analysis of the angular momentum composition of the calculated eigenfunctions enables us to determine the symmetries of the states around the gap at the Γ point of the folded Brillouin zone ("minizone"). The results can be used to assign two gaps observed in resonant Raman experiments.

The resonant Raman experiments have been performed for the GaAs-like and the AlAs-like optical phonons of $(GaAs)_1(AlAs)_1$. It is known that those phonons remain strongly confined to the GaAs and the AlAs layers, respectively, [at least for $n\geq2$ (Refs. 12–15)] and thus should correspond roughly in frequency to bulk phonons at the X point for the $(GaAs)_1(AlAs)_1$ superlattice. Besides these confined or nearly confined modes, nonconfined or "interface modes" have been recently observed in superlattices with $n,m\geq7$.[16,17] These are modes which propagate *parallel* to the interface. They are forbidden for backward scattering and thus can be observed only very close to resonance when the $\mathbf{k}$ conservation is lifted by impurities or surface roughness. Another possible mechanism for their observation is forward scattering by the beam reflected at the superlattice-substrate interface. These modes should appear between the TO and LO frequencies of the bulk materials.

Here we have looked for such modes in small period superlattices ($m\leq3$) and found no evidence of them at room temperature. We have observed, however, for $m=1,2$ satellites of the main LO phonon when the frequency of the exciting laser lies near 1.9 eV. These sa-

tellites appear at frequencies higher than the main LO modes. They are tentatively attributed to inverted Al-Ga pairs near the layer interfaces.

II. EXPERIMENT

The Raman measurements were performed with a SPEX Triplemate spectrometer using a multichannel detection system base on an ITT Mepsicron photodetector. The resolution of the system was 4 cm^{-1} at 2 eV. Discrete laser lines of Ar^+- and Kr^+-ion lasers were used and also, for detailed measurement of resonance profiles, a Coherent Radiation cw dye laser operated with the dyes Rhodamine-6G (2.1-eV region) and DCM [(1.9-eV region)].[18] At low temperatures the Raman spectra were swamped by strong luminescence. Hence, we performed all our measurements at room temperature.

The $(GaAs)_1(AlAs)_1$ superlattices were grown on a (001)GaAs substrate by MBE in the manner described in Ref. 19. They were part of a series of ultrathin-layer $(GaAs)_m(AlAs)_m$ superlattices with $1 \leq m \leq 10$, which were grown by molecular-beam epitaxy (MBE) and carefully characterized by x-ray diffraction and low-temperature photoluminescence (PL) measurements (see the Appendix).[20] The growth rates of GaAs and AlAs monolayers were accurately controlled by the period of the intensity oscillations of the specularly reflected beam in the reflection high-energy electron diffraction (RHEED) pattern. The formation of high-quality layered crystals is confirmed by the appearance of distinct satellite peaks around the (002) and (004) reflections of the x-ray diffraction pattern. The PL spectra of the ultrathin-layer $(GaAs)_m(AlAs)_m$ superlattices are in marked contrast to those obtained from the ternary $Al_{0.5}Ga_{0.5}As$ alloy grown in a different run under the same growth conditions. While the ternary alloy shows three PL lines, the no-phonon line, and two phonon sidebands of approximately the same intensity, the superlattices exhibit one strong PL line which shifts strongly in energy as a function of superlattice period. The luminescence of the $(GaAs)_1(AlAs)_1$ monolayer superlattice has a maximum at 1.93 eV, which is about 140 meV lower in energy than the no-phonon line of the ternary alloy of the same composition. This result for the monolayer superlattice is in good agreement with band-structure calculations.[1,3]

III. RESULTS

The Raman spectra measured with three different Ar^+- and Kr^+-ion laser lines ($\omega_L = 1.916$, 2.182, and 2.409 eV) are displayed in Fig. 1. As shown in Fig. 2 the spectrum for $\omega_L = 1.916$ eV corresponds to the top of a resonance peak, while that for 2.182 eV is slightly above resonance. The spectrum taken with $\omega_L = 2.409$ eV is nonresonant. The 1.916 eV data of Fig. 1 display two distinct peaks in the LO (GaAs) region and a peak with a shoulder in the LO (AlAs) region. These doublets are similar to those reported in Ref. 17 for $m = n = 2$ and larger period superlattices.

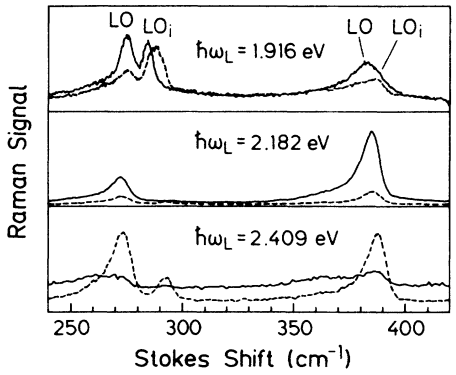

FIG. 1. Raman spectra of $(AlAs)_1(GaAs)_1$ in the region of LO GaAs-like and AlAs-like vibrations obtained with three different laser frequencies at room temperature. The solid line represents incident and scattered polarizations parallel to the same crystal axis, the dashed line represents polarization parallel to two different crystal axes.

At the other two excitation frequencies only the lower of the two pairs of structures is seen clearly [at ~ 273 cm^{-1} for LO (GaAs), ~ 386 cm^{-1} for (AlAs)]. The peak observed at 292 cm^{-1} for $\omega_L = 2.409$ eV corresponds to the LO phonon of the GaAs substrate. For the resonant spectra, the depolarized component is weaker than the polarized one. The opposite is true for the nonresonant spectra. The resonance at 2.15 eV appears to be stronger than that at 1.93 eV. The former was observed at the same position even in poorer quality samples (as characterized by x rays) while the latter depended rather critically on sample quality.

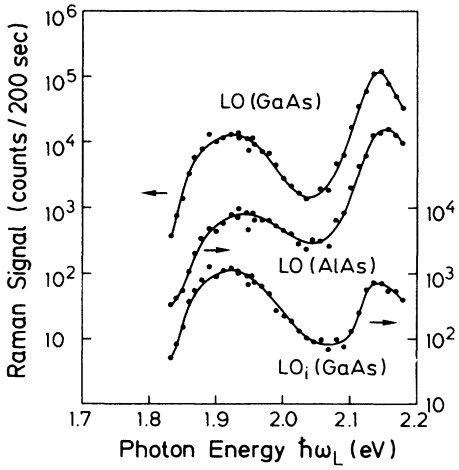

FIG. 2. Resonances of the maxima of the structure shown in Fig. 2. Two resonance energies are seen for the LO GaAs-like and AlAs-like peaks and also for the LO_i mode of GaAs. The latter exhibits stronger resonance at ~ 1.9 than at ~ 2.5 eV.

IV. THEORY AND DISCUSSION

A. Electronic states

The band structure of $(GaAs)_1(AlAs)_1$ was calculated self-consistently using the Dirac relativistic formulation of the linear mulfin-tin-orbital (LMTO) method. We show in Fig. 3 the bands along the symmetry lines $\Gamma-R$ and $\Gamma-M$ of the tetragonal Brillouin zone which correspond to the $\Gamma-L$ and $\Gamma-X$ (parallel to the layer plane) of the fcc lattice (see Fig. 4). The Γ-R directions of the "minizone" correspond, if the two metal atoms are the same, to the $\Gamma-L$ and $\Gamma-X$ directions of zinc blende (the latter perpendicular to the plane of the layers). The calculation proceeded along the lines of Ref. 5 except that the δ-function-like external potentials were added at the center of the atomic spheres, including the empty spheres. These potentials have the form[11]

$$V(r)=V_0\frac{r_0}{r}e^{-(r/r_0)^2} . \tag{1}$$

We list in Table I the values of the parameters V_0 and r_0 which gave good fits to the Γ (direct), L, and X (indirect) gaps of GaAs and AlAs. We were able to keep the same parameters for As and the empty spheres surrounded by As in both materials.

We list in Table II the energies of the three top valence bands and those of the six lowest conduction bands at Γ for $(GaAs)_1(AlAs)_1$ as obtained by the LMTO method after adding the potentials of Eq. (1). We have also listed the energies of the corresponding states for zinc-blende-type GaAs and AlAs calculated with the additional potentials of Table I. The correspondence is easily derived by looking at the angular momentum composition around the three atoms and the corresponding empty spheres (Table III). The valence bands are composed mainly of As $4p$ functions (60%), the highest being of pure Γ_5 orbital symmetry (x,y), which is the $(\frac{3}{2},\pm\frac{3}{2})$ band in angular momentum notation. The second and third highest valence bands are mixed Γ_5 and $\Gamma_3(z)$, i.e., they correspond to the $(\frac{3}{2},\pm\frac{1}{2})$ and $(\frac{1}{2},\pm\frac{1}{2})$ angular momentum states. (Note that our Γ_3 is labeled Γ_4 in Refs. 4 and 6. We prefer here the label Γ_3 so as to agree with the conventional X_3 notation for the X point of zinc blende.) The two upper valence bands are nearly degenerate (splitting 20 meV), the third is split from those by 330 meV, nearly the same spin-orbit splitting as for GaAs and AlAs.

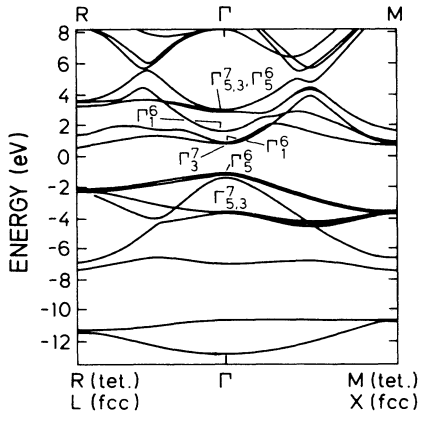

FIG. 3. Band structure of $(AlAs)_1(GaAs)_1$ calculated with the LMTO method with correction for the "gap problem" as indicated in the text.

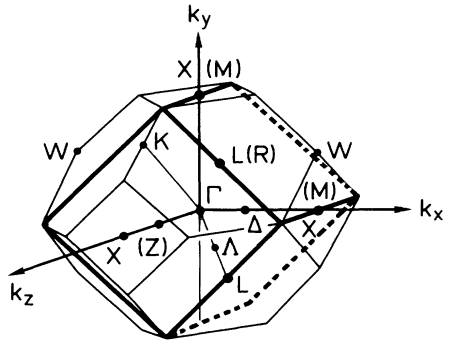

FIG. 4. Brillouin zone of the fcc lattice and, inscribed in the fcc lattice as thick lines, Brillouin zone (BZ) of the tetragonal lattice of $(AlAs)_1(GaAs)_1$. The symmetry point notation of the tetragonal BZ is given in brackets, that of the fcc BZ without brackets.

The 20 meV "crystal-field" splitting of the top valence bands may be changed by a slight mismatch in the lattice constant of GaAs (5.653 Å) and AlAs (5.660 Å)[21] (the calculations were performed for the same lattice constant of 5.653 Å, i.e., that of bulk GaAs). The effect of this mismatch strain has not been calculated in detail. It is, however, easy to estimate it. If we assume that the GaAs layers are not strained because of the influence of the GaAs substrate we obtain as correction the Γ_5-$\Gamma_{5,3}$ splitting:

$$\Delta(\Gamma_5\text{-}\Gamma_{5,3})=\delta\left[1+\frac{2C_{12}}{C_{11}}\right]b , \tag{2}$$

where b is the shear deformation potential of the Γ_8 band of AlAs, C_{ij} the elastic stiffness constants, and δ the lattice constant mismatch $\Delta a_0/a_0$ of AlAs with respect to GaAs ($\delta<0$). Equation (2) includes the fact that both AlAs and GaAs contribute nearly equally to the valence bands, i.e., the splitting that would obtain in bulk AlAs has been divided by two. Replacing into Eq. (2) the known values of b (-1.9 eV for GaAs, we take the same for AlAs) and $(2C_{12}/C_{11})=0.9$ for GaAs, 0.85

TABLE I. Parameters of the potential of Eq. (1) used in the present work to correct for LDA errors in the gaps. V_0 is in hartrees (27.2 eV) and r_0 in bohrs.

				Empty spheres		
	As	Ga	Al	As_1, As_2	Ga	Al
V_0	190	280	340	6	5	5
r_0	0.015	0.015	0.015	0.55	0.55	0.55

TABLE II. Energies of the three top valence bands and the six lowest conduction bands of $(GaAs)_1(AlAs)_1$, GaAs, and AlAs obtained with the LMTO method with correction of LDF errors effected by potentials of the type of Eq. (1) with the parameters given in Table I. The irreducible representation of the D_{2d} structure is given followed by the corresponding zinc blende representations. The energies are referred to the natural ASA scale in which the Coulomb potential of the atomic spheres is zero at infinity.

	$\Gamma_{5,3}^7$ Γ_4^7	$\Gamma_{5,3}^7$ Γ_4^8	Γ_5^6 Γ_4^8	Γ_3^7 X_3^7	Γ_1^6 X_1^6	Γ_1^6 Γ_1^6	$\Gamma_{5,3}^7$ Γ_4^7	Γ_5^6 Γ_4^8	$\Gamma_{5,3}^7$ Γ_4^8
$(GaAs)_1(AlAs)_1$	−1.51	−1.19	−1.17	0.75	0.78	1.57	2.81	2.93	2.94
GaAs	−1.44	−1.09	−1.09	1.14	0.82	0.31	2.57	2.78	2.78
AlAs	−2.08	−1.76	−1.76	0.99	0.20	1.15	2.61	2.64	2.64

for AlAs (Ref. 21) we find $\Delta(\Gamma_5-\Gamma_{5,3})\approx+4$ meV, i.e., the splitting would increase only slightly. If the memory of the substrate lattice constant a_0 is lost, due to the formation of dislocations (i.e., in our case, the presence of vacancies), the strain effects on AlAs ($\delta<0$) would cancel those on GaAs ($\delta>0$).

Before applying the potentials of Eq. (1) and Table I the lowest conduction band state of the superlattice was the counterpart of the lowest conduction band state of GaAs. The application of the adjusting potentials lifts this Γ_1^6 state more than the Γ_3^2 state which becomes the lowest. The energy difference between these states, however, is rather small (30 meV) and, since Γ_1 and Γ_3 have different symmetries, a small perturbation may reverse their order. Thus we cannot rely on our calculations to establish this order. The resonance data of Fig. 2, however, support the calculated ordering although the measured Γ_1-Γ_3 splitting (218 meV, see below) would be larger than the calculated one. We find this difference between theory and experiment acceptable in view of the vagaries of our correction to the LDA.

The optical matrix elements for the valence to Γ_3 transition should be much smaller than those for transitions to the lowest Γ_1 states. This is a carryover of the $\Gamma_8\rightarrow X_3$ forbidden transition of zinc blende. In fact, in the $(GaAs)_1(AlAs)_1$ structure the Γ_3 transitions should

TABLE III. Angular momentum decomposition (in %) of the wave functions around the As, Ga and Al spheres, and also the empty spheres inside of As and Al-Ga tetrahedra, as obtained with the LMTO method. The energy of the state with respect to the top of the valence band is given in eV under its irreducible representation. The atomic and empty sphere coordinates are (in units of $a_0/2$) As(1,0,$2^{-1/2}$), (0,1,3×$2^{-1/2}$), Ga(0,0,0), Al(1,1,$2^{1/2}$), As_1(0,0,$2^{1/2}$) As_2(1,1,0), Ga-Al(1,03×$2^{-1/2}$), (0,1,$2^{-1/2}$).

State and energy	Component	As	Ga	Al	Empty spheres As_1	As_2	Ga-Al
$\Gamma_{5,3}^7$	*s*	0	0	0	0	0	0.2
−0.34	*p*	68.9	6.7	4.5	0.1	0.3	2.4
	d	1.2	3.8	6.0	2.9	2.4	0.3
$\Gamma_{5,3}^7$	*s*	0	0	0	0	0	0.5
−0.02	*p*	67.3	7.4	4.3	0.1	0.3	2.5
	d	1.4	3.7	6.5	3.1	2.3	0.4
Γ_5^6	*s*	0	0	0	0	0	0
0	*p*	68.2	6.4	5.2	0.2	0.1	2.6
	d	4.0	4.2	5.9	2.7	2.7	0.4
Γ_3^7	*s*	7.1	0	0	0	0	41.1
+1.92	*p*	1.4	8.1	12.6	4.0	2.5	0
	d	10.6	5.0	3.5	1.8	3.3	0
Γ_1^6	*s*	25.9	33.2	3.2	8.0	3.0	8.5
+1.95	*p*	6.7	0	0	0	0	0.5
	d	4.5	1.1	2.1	0.1	0.3	2.6
Γ_1^6	*s*	13.4	0	30	6.0	14.0	6.9
+2.74	*p*	7.0	0	0	0	0	0.4
	d	9.9	2.1	4.0	0.4	0.7	5.3
$\Gamma_{5,3}^7$	*s*	0	0	0	0	0	0
+3.98	*p*	4.3	25.6	24.9	6.5	6.1	4.8
	d	15.8	0.6	0.8	1.0	0.8	8.8
Γ_5^6	*s*	0	0	0	0	0	0
+4.10	*p*	4.6	25.2	24.2	6.5	6.3	4.9
	d	15.9	0.6	0.9	0.9	0.9	8.9
$\Gamma_{5,3}^7$	*s*	0	0	0	0	0	0
+4.11	*p*	4.6	24.7	24.8	6.8	6.1	4.9
	d	15.9	0.6	0.9	1.0	0.9	8.9

become allowed mainly because of the difference in Al p and Ga p compositions of the Γ_3 state (Table III). The corresponding matrix element can be estimated to be, using the data of Table III

$$\langle \Gamma_5^x \mid p_x \mid \Gamma_3 \rangle \approx 10^{-2}[\sqrt{68}(\sqrt{12.6}-\sqrt{8.1})]Q = 0.06Q \ , \quad (3)$$

where Q is the Γ_5 (valence)$\rightarrow\Gamma_5$ (conduction) matrix element of zinc blende [$Q \approx 0.5$ a.u. (Ref. 22)]. For the $\Gamma_5\rightarrow\Gamma_1$ transitions we estimate in a similar manner:

$$\langle X_5^x \mid p_x \mid \Gamma_1 \rangle = 10^{-2}[\sqrt{68}(\sqrt{33.2}+\sqrt{12.7})]P = 0.62P \ , \quad (4)$$

where $P \approx 0.6$ a.u. Thus we see that the matrix element of Eq. (4) is one order of magnitude larger than that of Eq. (3), and the oscillator strength for transitions to Γ_3 should be 2 orders of magnitude smaller than that for transitions to Γ_1. The larger effective mass of the Γ_3 minimum, however, should enhance the strength of the weak Γ_3 transitions which will, nevertheless, remain weaker than those to Γ_1. Thus we assign to the former the weak-resonance peak of Fig. 2 (1.93 eV) and to the latter the stronger one (2.15 eV). The reversal of the Γ_1-X_3 order of GaAs in $(GaAs)_m(AlAs)_m$ for $m=1$ can be understood as related to the large increase in the Γ_1 minimum with decreasing m (quantum well effect) while this effect is absent for the X_3 minima because of the absence of a barrier. Hence a crossing must occur (see Ref. 1) approximately for $m=2$ or 3. One may argue, however, that the Γ_3 minima under consideration contain, according to Table II, a mixture of Al and Ga p functions with predominance of the former for which there may be an energy barrier. Nevertheless, the masses at X_3 are so large that confinement effects on the energy should be negligible. Other available calculations also reproduce the Γ_3-Γ_1 ordering found here.[1-4]

Some effort should be made to detect transitions to the third lowest Γ_1 conduction state, mainly Al $3s$-like, which should yield a transition matrix element of the order of that of transitions to the lower Γ_1. The transitions should occur around 2.7 eV (Table III).

We have not been able to resolve the transitions from the two top valence bands ($\Gamma_{5,3}^7$ and Γ_5^6) and thus to determine their ordering, although we believe that the theoretical results should be reliable (note that $\Gamma_{5,3}^7$ and Γ_5^6 correspond to $(\frac{3}{2},\pm\frac{1}{2})$ and $(\frac{3}{2},\pm\frac{3}{2})$, respectively, in angular momentum notation). The reason for our failure is that we are only observing transitions polarized in the plane of the layers. In this case the $(\frac{3}{2},\pm\frac{3}{2})$ states should give the larger contribution.[22] Observation of emission (luminescence or light scattering) along the plane of the layers, as done in Ref. 23 for larger values of m, should help resolve the splitting and establish the ordering of the Γ_5-$\Gamma_{5,3}$ states (especially if these measurements are performed at low temperatures).

We note that the resonances of Fig. 2 peak at slightly lower energies for the GaAs phonons (1.922, 2.142) than for those in AlAs (1.940, 2.156). The difference, 16±2 meV, is rather close to the difference between the phonon frequencies of GaAs and AlAs (14 meV according to Table IV). This suggests that the resonances occur when the photon energy of the *scattered* photon equals that of the gaps (outgoing resonance). This phenomenon is typical of defect-induced resonance in the scattering by LO phonons.[23,24] If this situation applies, one would have to subtract the phonon energy from the energies of

TABLE IV. Compilation of wave numbers (cm^{-1}) of Raman structures observed at 300 K for $(AlAs)_m(GaAs)_n$ with $m=n=1,2,3$. The symbol $\parallel$ represents incident and scattered polarizations parallel to the same crystal axis while $\perp$ represents polarizations parallel to two different crystal axes. The LO phonons of the bulk materials were found to be at 291.5 (GaAs) and 402 (AlAs) cm^{-1}. The LO_i modes are assigned in the text to Ga-Al pairs.

	Superlattice	$\hbar\omega_L$ (eV)	LO,$\parallel$	LO,$\perp$	LO_i,$\parallel$	LO_i,$\perp$
GaAs region	$m=n=1$	1.916	275.3	275.8	284.5	287.5
		2.182	271.5	271.5		
		2.409	273.5	273.1		
	$m=n=2$	1.916	277.3	278.1	285.3	287.5
		2.182	275.0	278.5		
		2.409	276.0	278.7		
	$m=n=3$	1.916	283.1	283.1		
		2.182		283.1		
		2.409	284.0	284.2		
AlAs region	$m=n=1$	1.916	385.8		390.5	390.5
		2.182	384.6	384.6		
		2.409	387.4	387.4		
	$m=n=2$	1.916	384.4			
		2.182	384.7			
		2.409	387.5			
	$m=n=3$	1.916				397
		2.182	382.3	381.6		394
		2.409				394

the resonant peaks to obtain the corresponding gaps. This would lead to 1.890 and 2.108 eV for $\Gamma_{5,3}\rightarrow\Gamma_3$ and $\Gamma_{5,3}\rightarrow\Gamma_1$ gaps, respectively (compare with the calculated 1.92 and 1.95 eV given in Table III).

B. Phonons

We have shown in Fig. 1 that in the nonresonant situation (2.41 eV) the configuration with crossed polarizations $\perp[z(x,y)\bar{z}$ in standard notation] gives the dominant spectra. This is expected from the Γ_3 (B_2 in molecular notation) symmetry of the corresponding LO phonons. The $\parallel$ configuration $[z(x,x)\bar{z}]$ should only couple *in the dipole approximation* to phonons of Γ_1 and Γ_2 symmetry[12] which do not exist in this region for the $m=n=1$ superlattices. Γ_1 phonons have been seen to resonate rather strongly in the $\parallel$ configuration in superlattices with $m=n=7$ for which the electron states are completely localized in the GaAs layers.[15,16] For smaller values of m and n, for which band formation along the z direction takes place, the standard forbidden intraband Fröhlich mechanism can make the Γ_3 vibrations allowed near the resonance in $\parallel$ configuration.[25] This is seen in Fig. 1: both AlAs- and GaAs-like phonons not only appear in $\parallel$ configuration under resonant excitation but they become dominant. Most conspicuous is the appearance of a second structure above the main Γ_3 phonon but below that of the bulk compound ($\sim$286 cm^{-1}, 390.5 cm^{-1}). This structure cannot be assigned to any phonon propagating along z. We have thus considered assignment to phonons propagating perpendicular to z. Such phonons can be treated as vibrations of an average material, with an average dielectric constant $\epsilon=\frac{1}{2}(\epsilon_{\mathrm{GaAs}}+\epsilon_{\mathrm{AlAs}})$ and are often referred to as "interface modes."[12,13,17] Setting this dielectric constant equal to zero one obtains longitudinal modes propagating perpendicular to z. Such modes have been observed[12,17] for $m,n\geq 4$ where they fall between the first confined LO and TO modes. For smaller period superlattices the electrostatic treatment should break down and one can conjecture that the "interface modes" fall above the first LO mode since the interface modes are related to the LO-TO modes of the bulk material at $k\approx 0$ while the allowed LO mode is basically an edge-of-the-zone mode. However, recent lattice dynamical calculations based on the shell model[26] have shown this not to be the case for $m=n=1-5$. We note that the high-frequency satellite is also observed for $m=n=2$ (see Ref. 27) but not for $m=n=3$ (Table IV). We are thus led to an interpretation of the satellites in terms of imperfections of the superlattices, which, anyway would also be required to couple to the "interface modes" in backscattering.

Probably the most likely type of defect is a reversal of a second neighbor Ga-As pair. This would produce, for the $m=n=1$ superlattice, Ga-As-Ga and Al-As-Al units which would be expected to yield local vibrational modes at frequencies closer to those of the bulk (thus higher than the LO's of the perfect superlattices). For $m=n>1$ the reversal would be most likely to occur about the As interfaces. For $m=n\geq 3$ the number of reversed pairs should be smaller than in the $m=n=1,2$ cases. This may explain the lack of satellites in these cases. Until further work is performed this conjecture must be taken as tentative.

It is interesting to note that both GaAs- and AlAs-like modes resonate with nearly the same strength at both resonances. This may appear somewhat strange when one considers that the $\Gamma_{5,3}\rightarrow\Gamma_1$ gap ($\sim$2.15 eV) is GaAs-like. For a larger period superlattice under these conditions only the GaAs phonon modes would resonate at a GaAs-like gap. However, in the case of the Γ_3 mode of an $m=n=1$ superlattice *all* As atoms move with nearly the same amplitude for both AlAs- and GaAs-like modes. Hence both types of modes should "modulate" both GaAs- and AlAs-like gaps and thus resonate at them.

The wave numbers of all peaks observed in Fig. 1 are listed in Table IV, together with the results of similar measurements for superlattices with $m=n=2$ and $m=n=3$. We note that there are small changes in the wave number of a given structure when observed with different laser lines. No systematic study of such variation has been performed.

V. CONCLUSIONS

In a $(\mathrm{GaAs})_1(\mathrm{AlAs})_1$ superlattice we have observed resonances of the Raman scattering by GaAs- and AlAs-like LO phonons. The resonance maxima are identified to be "outgoing resonances." On the basis of LMTO band structure calculations the corresponding resonant gaps at 1.890 and 2.108 eV, at room temperature, are assigned to transitions from the top valence band to the Γ_3 and Γ_1 conduction bands, respectively. At the Γ_3 resonance, additional peaks appear which can be tentatively assigned to reversed Ga-Al second-neighbor pairs.

ACKNOWLEDGMENTS

We would like to thank H. Hirt, M. Siemers, and P. Wurster for expert technical assistance, and D. S. Jiang for illuminating discussions. One of us (T.S.) thanks the A. von Humboldt Foundation for support.

APPENDIX

In this appendix we present some results to illustrate the quality of our ultrathin-layer $(\mathrm{GaAs})_m(\mathrm{AlAs})_m$ superlattices used here. The crystal quality and the superlattice period were determined from x-ray rocking curves using a high-resolution double-crystal x-ray diffractometer[27] and also a counter diffractometer for a rapid scan over a wide range of diffraction angles. The diffraction patterns were recorded in the vicinity of the (002) and the (004) reflection using Cu $K\alpha$ radiation. In Fig. 5 we show the measured x-ray diffraction curves for the $m=1$, 2, and 3 superlattices. In this figure the (002) peak at $\theta=15.8°$ as well as the (004) peak at $\theta=33.0°$ originate from both the epitaxial layer and the substrate. The weak (± 1) satellite reflections on the higher and lower angle side of these two Bragg reflections clearly indicate the existence of periodic structures. The period D of the $(\mathrm{AlAs})_m(\mathrm{GaAs})_m$ superlattices can be determined

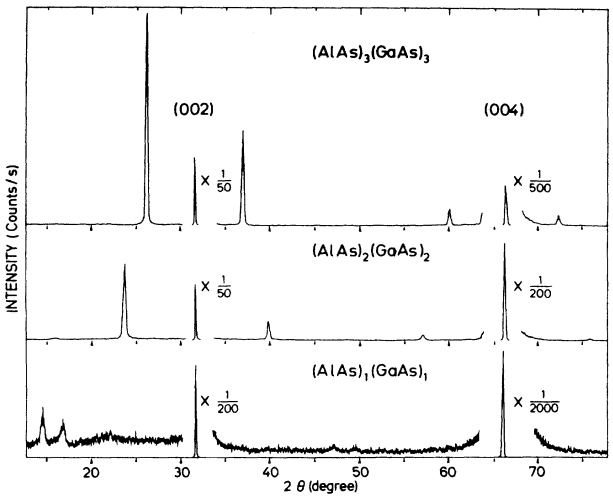

FIG. 5. X-ray diffraction curves of $(GaAs)_m(AlAs)_m$ superlattices with $m=1$, 2, and 3 obtained in the vicinity of the (002) and (004) Bragg reflections using Cu $K\alpha$ radiation.

from the angular distance between the zeroth-order (002) or (004) peak and the respective ($\pm$) satellite peaks using the equation

$$D=\frac{\lambda}{2\,|\,\sin\theta_{(\pm1)}-\sin\theta_0\,|}\ , \tag{A1}$$

where λ is the x-ray wavelength and $\theta_{(\pm1)}$ and θ_0 are the diffraction angles of the first-order satellite and of the zeroth-order reflection, respectively. Precise measurements of the angular separation $\Delta\theta_{0,s}$ between the substrate diffraction peak and the zeroth-order diffraction peak of the superlattice by means of the double-crystal x-ray diffractometer yield the average value of the lattice constant and the average value of the Al composition x of the epitaxial layer, i.e., of the $(GaAs)_m(AlAs)_m$ superlattice by applying Vegard's rule similar to the case of the ternary $Al_xGa_{1-x}As$ alloy.[27] While for the $m=3$ and $m=2$ superlattices distinct ($\pm$) satellite peaks are located at the expected angular position, we observe a splitting of the satellite peaks for the $m=1$ superlattice. Two peaks appear around the ideal (001) position at $\theta=7.827°$ ($2\theta=15.654°$) as well as around the ideal (003) position at $\theta=24.11°$ ($2\theta=48.22°$). This splitting implies a slight deviation of the superlattice period D from the ideal (twice the lattice constant a). From a careful evaluation of the RHEED intensity oscillation patterns we assume that the period length of the $(AlAs)_1(GaAs)_1$ superlattice might be larger by about 5 to 8% as compared to the ideal value of 5.659 Å. In this case each of the two satellite peaks located closer to the (002) and to the (004) reflection belongs to the respective zeroth-order peaks.

TABLE V. Variation of photoluminescence peak energy as a function of period length observed in ultrathin-layer $(AlAs)_m(GaAs)_m$ superlattices kept at 2 K. For comparison, also the energy of the bound-exciton luminescence detected in the ternary $Al_xGa_{1-x}As$ alloy is included.

Superlattice configuration	Average Al composition x	Luminescence peak energy (eV)
$(AlAs)_1(GaAs)_1$	0.51	1.931
$(AlAs)_2(GaAs)_2$	0.51	1.968
$(AlAs)_3(GaAs)_3$	0.49	2.033
$(AlAs)_4(GaAs)_4$	0.49	1.964
$Al_xGa_{1-x}As$ alloy	0.52	2.077

The low-temperature photoluminescence spectra obtained from the four prototype ultrathin-layer $(GaAs)_m(AlAs)_m$ superlattices with $m=1$, 2, 3, and 4 are dominated by a strong luminescence line which shifts in energy as a function of period length, i.e., of m. In Table V we have summarized the luminescence peak energies of the four superlattices. For comparison we have also included the peak energy of the bound exciton ("no-phonon") line from the ternary $Al_xGa_{1-x}As$ alloy. Although all five sample configurations were prepared under similar MBE growth conditions and have nearly the same average composition of $Al_{0.5}Ga_{0.5}As$, distinct differences exist in the peak position and in the line shape of the observed luminescence. The important result is that except for the ternary alloy the $m=3$ superlattice exhibits the highest luminescence peak energy of all $(GaAs)_m(AlAs)_m$ superlattices. In particular the luminescence of the monolayer superlattice is shifted by 146 meV to lower energy as compared to the ternary $Al_{0.52}Ga_{0.48}As$ alloy.[20]

*On leave from Tohoku University, Sendai, Miyagi 980, Japan.
†Permanent address: Central Research Laboratories, Mitsubishi Electric Corporation, Tsukaguchi-honmachi, Amagasaki, Hyogo 665, Japan

[1]M. A. Gell, D. Ninno, M. Jaros, and D. C. Herbert, Phys. Rev. B **34**, 2416 (1986) and references therein.
[2]J. N. Schulman and T. C. McGill, Phys. Rev. B **19**, 6341 (1979).
[3]T. Nakayama and H. Kamimura, J. Phys. Soc. Jpn. **54**, 4726 (1985).
[4]W. Andreoni and R. Car, Phys. Rev. B **21**, 3334 (1980).
[5]N. E. Christensen, E. Molinari, and G. B. Bachelet, Solid State Commun. **56**, 125 (1985).
[6]E. Caruthers and P. J. Liu-Chung, J. Vac. Sci. Technol. **15**, 1459 (1978); Phys. Rev. Lett. **38**, 1543 (1977).
[7]W. E. Picket, S. G. Louie, and M. L. Cohen, Phys. Rev. B **17**, 815 (1978).
[8]A. Ishibashi, Y. Mori, M. Itabashi, and N. Watanabe, in *Proceedings of the International Conference on the Physics of Semiconductors,* edited by O. Engström (World Scientific, Singapore, 1987), p. 1365.
[9]M. S. Hybertsen and S. Louie, Phys. Rev. Lett. **55**, 1418 (1985).
[10]G. Baraff and M. Schlüter, Phys. Rev. B **30**, 3460 (1984).
[11]N. E. Christensen, Phys. Rev. B **30**, 5753 (1984).
[12]A. K. Sood, J. Menéndez, M. Cardona, and K. Ploog, Phys.

Rev. Lett. **54**, 2111 (1985).
[13]M. V. Klein, IEEE J. Quantum Electron. **QE-22**, 1760 (1986) and references therein.
[14]A. Ishibashi, M. Itabashi, Y. Mori, K. Kaneko, S. Kawado, and N. Watanabe, Phys. Rev. B **33**, 2887 (1986).
[15]B. Jusserand and D. Paquet, Phys. Rev. Lett. **56**, 1752 (1986).
[16]J. Menéndez, A. K. Sood, M. Cardona, and K. Ploog, Phys. Rev. Lett. **54**, 2115 (1985).
[17]C. Colvard, R. Merlin, M. V. Klein, H. Morkoc, A. Y. Cho, and A. C. Gossard, Phys. Rev. Lett. **45**, 298 (1980).
[18]These dyes were supplied by Lambda Physik, Göttingen.
[19]J. L. deMiguel, K. Fujiwara, L. Tapfer, and K. Ploog, Appl. Phys. Lett. **47**, 836 (1985).
[20]T. Isu, D. S. Jiang, and K. Ploog, Appl. Phys. A **43**, 75 (1987).
[21]*Landolt-Börnstein Tables,* edited by O. Madelung, M. Schulz, and H. Weiss (Springer, Heidelberg, 1982), New Series, Vol. 17a.
[22]M. Cardona, J. Phys. Chem. Solids **24**, 1543 (1963).
[23]J. E. Zucker, A. Pinczuk, D. S. Chemla, A. Gossard, and W. Wiegmann, *in Proceedings of the International Conference on Physics of Semiconductors,* edited by J. Chadi and W. Harrison (Springer, New York, 1985), p. 563.
[24]W. Kauschke and M. Cardona, Phys. Rev. B **33**, 5473 (1986).
[25]M. Cardona, in *Light Scattering in Solids II,* edited by M. Cardona and G. Güntherodt (Springer, Heidelberg, 1982), p. 128.
[26]E. Richter and D. Strauch (unpublished); thesis, University of Regensburg, 1986.
[27]L. Tapfer and K. Ploog, Phys. Rev. B **33**, 5565 (1986).